Effect of upstream velocity profile and integral flow straighteners on turbine flowmeters

L. A. Salami*

One of the most important factors determining the shape of the calibration curve for a given turbine meter is the change in the upstream velocity distribution with flowrate. A theoretical model is evolved which can be used to predict the effects of velocity profile, viscosity and swirl on the calibration curve. It has also been used to explain the calibration curve of a commercial meter having a geometry very different from that for which the theory was developed. The effect of different types of integral flow straighteners on turbine meters is also investigated and found to depend on both the number of vanes and their length. A correlation is suggested for radial-vaned flow-straighteners

Keywords: *flow measurement, turbine meters, flow straighteners*

In most of the existing literature on turbine-type flowmeters the velocity profile just upstream of the rotor blades is assumed uniform. To obtain, or at least approach this condition, rotors with high hub-to-tip ratio, ψ, are used in the majority of cases; although in some designs, such as the commercial meter referred to in this article, the rotor is mounted in a venturi. More often than not, these meters give an increase in meter coefficient, MC (defined here as pulses/kg of fluid) as the flow decreases, and are therefore inconveniently non-linear. Until now these increases in meter coefficient have been attributed[1] to the Reynolds number effect on the rotor losses.

Jepson[2] obtained a linear calibration curve even down to 10% of the maximum flowrate when he used a meter with a small hub and with a tip diameter just smaller than the pipe inside diameter, giving $\lambda = 0.0075$; this meter will be referred to as the small-tip-clearance rotor meter. However, this meter was susceptible to upstream velocity distribution. A theory based on aerofoil theory was used to predict that the effect of the upstream velocity distribution between uniform and fully developed flows could be eliminated by turning down the rotor of the meter to give $\lambda = 0.044$ and this was confirmed experimentally for the maximum flow. Later investigation by the author showed that the meter coefficient of this meter, to be referred to as large-tip-clearance rotor meter, increased with decreasing flowrate. Since the Reynold's number range is roughly the same for both meters, the increase in meter coefficient with flowrate for some meters cannot be due to Reynolds number effects on the blades. An attempt is made here to explain that result by proposing a new theoretical model for turbine meters as the existing models[1-4] did not explain the results adequately.

An investigation of the effect of developing pipe flow on the meter has been carried out using three flowrates instead of the single flow rate used by Jepson[2]. The results are described in this article with the results of similar investigations on a commercial meter to see whether the new model will also explain its behaviour.

* Mechanical Engineering Department, University of Benin, Benin City, Bendel State, Nigeria

Received 15 April 1983 and accepted for publication on 23 February 1984

Effect of integral flow straightener

There are generally two types of flow straightener that are used to remove swirl upstream of the rotor of the meter. These are the in-line flow straightener which is generally installed in the pipe some distance upstream of the meter, and the integral flow straighteners which are usually placed just before and just after the rotor of the meter and are integral parts of the meter. It is the effect of the latter type of flow straightener that is now being considered here.

Integral flow straighteners not only perform the primary and very important function noted above but also serve the secondary purpose of housing the bearing. Their proximity to the rotor, as a consequence of the latter function, is therefore, usually unavoidable. Being so close, they present a distorted flow to the rotor because the area of the flow passage is occupied by the wake coming from the straightener. Thus an integral flow straightener is likely to affect the calibration of a turbine flowmeter. If two different types of flow straightener are used with the same rotor the result may be slightly different.

Many types of flow straightener are used by various turbine flowmeter manufacturers. It is obvious that if they are too short they are unlikely to be effective whatever their shape. On the other hand, very long flow straighteners increase both the capical cost of the meter due to the longer overall length, and the running cost due to the much increased frictional losses in them. It is, therefore, important that the flowmeter should be just long enough to remove the swirl completely.

This paper aims to both throw more light on the effect of integral flow straighteners on turbine flowmeters and to evolve a criterion to measure the effectiveness of a straightener.

Experimental details

The test rig (Fig 1) uses a 50.8 mm diameter test length. The velocity is almost uniform at the start of the test length but fully developed towards its downstream end. The small-tip clearance and the large-tip clearance meters were calibrated in the almost uniform and fully developed flows (Fig 2).

The meters were also tested at various positions in the developing flow in the test length at three flowrates. Fig 3 shows the mean curves through the experimental points of the three flowrates. The flowrates, which were chosen to lie in the linear region of the characteristic curves for the meter with small-tip clearance both in the uniform as well as in the fully developed flow, are shown in Fig 2. They are designated low, medium and high.

A similar test programme was carried out on a 38 mm commercial meter having a large-tip clearance $\lambda=0.10$ and the rotor with a 12.7 mm diameter hub mounted in the 25.4 mm diameter venturi throat of the casing. The test length used in this meter was 38 mm diameter bore. Only the calibration curves are reproduced here in Fig 4 as the meter showed very little upstream velocity profile effect.

Integral flow straighteners

These experiments were carried out in the constant head rig shown in Fig 1. Swirl was produced by a swirl generator which consists of a flanged piece of pipe with 50.8 mm internal bore with four identical, individually controlled flat blades inside the bore. When the planes of the blades are inclined at an angle to the direction of the flow, swirl is generated.

Notation

- a,a_i Angle of incidence (or attack) on rotor blade element; a_i induced angle
- A Area of meter based on the internal bore radius, R_0
- A_h Area of the meter hub, πR_h^2
- AR Aspect ratio of rotor blades
- $B,\bar{B}$ Constants pertaining to leakage flow
- B_g A function of speed which takes the effect of rotation of the rotor on the rotor blockage effect into accound
- c Blade chord
- C_D, C_{Do} Coefficient of profile drag; C_{Do} is C_D at $a=0$
- CF Conversion Factor $=MC/W$ at fully developed turbulent pipe flow
- C_L Coefficient of lift, proportional to sin a
- D Drag on rotor blade element; also represents diameter of 25 cm pipe in the calibration rig, Fig 1
- d Test pipeline inside diameter
- F,F_s Function of AR and τ; F_s function for correlating effects of flow straighteners
- k,K, $\bar{k}$ Constants pertaining to bearing loss
- L Lift on rotor blade element
- L_s Length of flow straighteners
- $l,\bar{l}$ Overall axial length of rotor; $\bar{l}$ non-dimensional overall axial length of rotor l/R_0
- m,m_e Constant of proportionality in the formula for C_L above; m_e effective value of m
- MC Meter coefficient, pulses/kg or pulses/litre
- N Number of blades on rotor
- N_s Number of vanes in the integral flow-straightener
- n Exponent in the velocity power law $\bar{U}=(1-\bar{r})^{1/n}$
- p Blade pitch
- $r,\bar{r}$ Radial distance of any point from the pipe centre; $\bar{r}$ non-dimensional radial distance r/R_0
- Re Reynolds number of blade or plate, $V_r c/\nu$
- Re_d Pipe Reynolds number, $U_0 d/\nu$
- R_0, R_h Meter inside radius at the position where the rotor is mounted; R_h radius of hub
- s Spacing between rotor blades
- T Torque on rotor
- t Blade thickness
- t_c Rotor tip clearance
- U_c Uniform axial velocity at the centre of the pipe in developing pipe flow; also velocity at the centre of the pipe
- U_0 Mean velocity across the pipe section
- U_r,U_r^* Axial velocity at a point r from the pipe axis just in front of the rotor; U_r^* axial velocity already corrected for blockage due to the hub
- $\bar{U}$ Non-dimensional axial velocity, U_r/U_0
- V_L Leakage velocity at right angles to the chord of the blade element at the blade tip
- V_r Absolute velocity in front of the rotor at a point r from the pipe axis
- $\bar{V}_r$ Relative velocity of the fluid to the blade
- W Non-dimensional meter coefficient, $\omega_R R_0/U_0$
- W_s Non-dimensional swirl velocity, $\omega_s R_0/U_0$
- y Distance of any point from the wall, R_0-r
- β Angle which $\bar{V}_r$ makes with the axial direction
- $\delta,\bar{\delta}$ Boundary layer thickness; $\bar{\delta}=\delta/R_0$
- ε Relative error, ie percentage change near zero swirl of the meter characteristics relative to its characteristic at zero swirl per degree of swirl generated
- λ Tip clearance ratio t_c/R
- μ Dynamic viscosity of liquid
- ν Kinematic viscosity of liquid
- ρ Density of liquid
- τ Parameter taking into account blade geometry (planform, twist, etc)
- ϕ Blade angle, ie angle which the rotor blade makes with the pipe axis
- ψ Hub ratio of rotor
- ω_R, ω_{R^*} Rotor angular velocity; ω_{R^*} rotor angular velocity at 'high' flowrate
- ω_s Angular velocity at any point in the pipe due to swirl

Subscripts

- b Bearing
- d Driving
- r Value of a parameter at a particular radial distance r
- s Swirl
- $\bar{s}$ Secondary and leakage flow losses
- t Tip

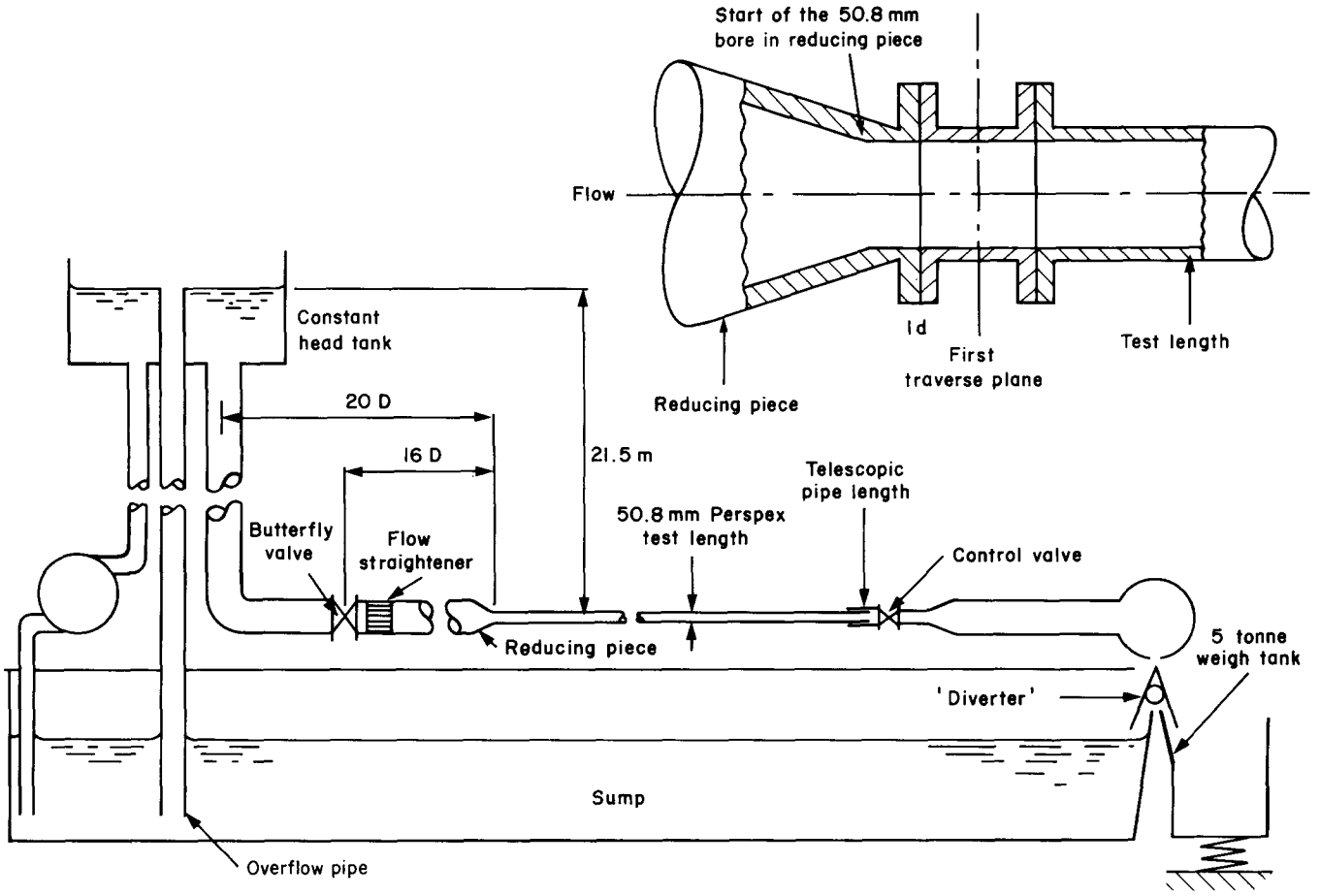

Fig 1 Layout of the constant head calibration rig. Details of the entry section demonstrate why it is impossible to obtain absolutely uniform flow in this rig

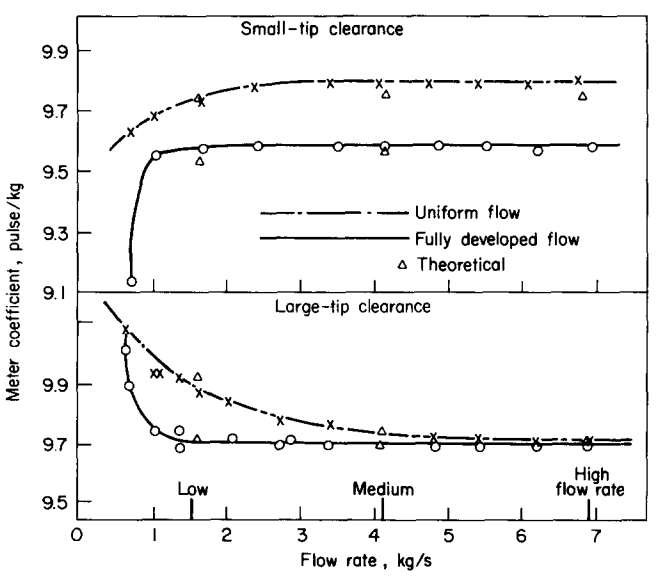

Fig 2 Calibration curves for both small- and large-tip clearance meters

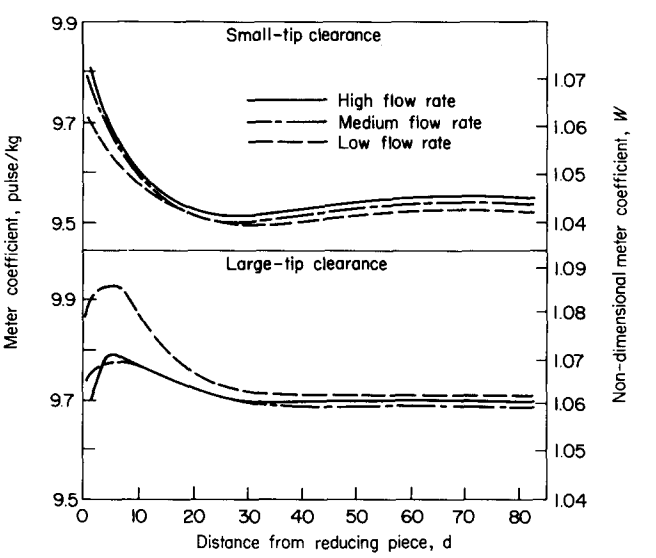

Fig 3 Upstream velocity effect. Mean experimental curves are shown

Previous work has shown that the swirl produced is not uniform but its magnitude at any point is approximately proportional to the blade setting of the generator up to about 15°. Thus, the setting of the blade could be used to give the magnitude of the swirl produced.

The swirl generator is mounted upstream of the meter and a perspex spacer into which the flow straighteners are inserted separates the two (Fig 5). Basically, two types of flow straightener were investigated: radial-vaned and ringed types. While only the four-ringed type was tested, the number of vanes in the radial type was varied. The length of the straightener was also changed; Table 1 gives the main parameters.

With the arrangement in Fig 5 and using the flow straighteners in turn, the meter coefficient was obtained

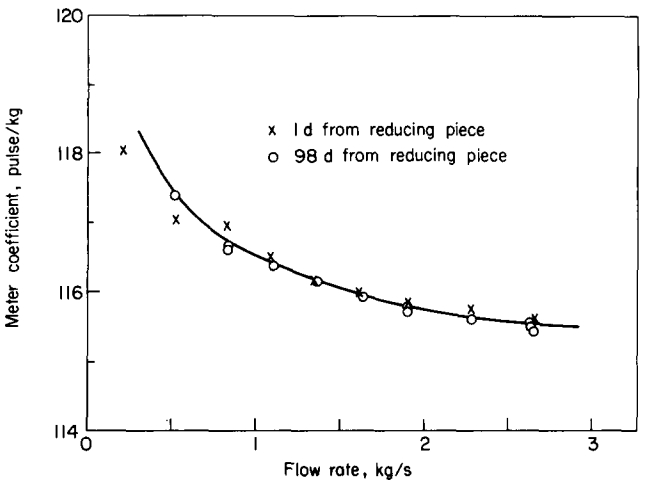

Fig 4 Calibration curve for the commercial meter demonstrating typical behaviour for many meters, with the meter coefficient increasing with decreasing flow rate. Note that there is no substantial profile effect

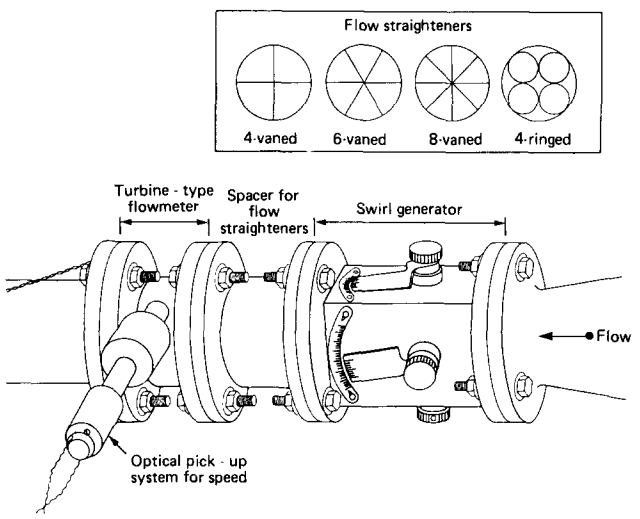

Fig 5 Typical layout for investigations into the effect of flow straighteners on meter characteristics

for various generator settings. The investigation was carried out in the uniform and the fully developed flows.

The meter coefficient for the meter without flow straightener is plotted in Fig 6 for the uniform flow. The same graph shows the result obtained using the 12.5 mm long four-vaned flow straightener. There is a drastic reduction in the effect of swirl on the meter. The curves are almost linear close to zero swirl and a relative error, ε, can thus be defined for small swirls as the percentage change of the meter characteristic relative to its characteristic at zero swirl, per degree of swirl generated. Whether ε is positive or negative will depend on the sign of swirl generated. Positive swirl is defined as the swirl in the direction of rotation of the rotor while upstream of the rotor.

Fig 6 shows the efficacy of the 4-, 6- and 8-vaned flow straighteners in removing swirl. These are typical figures for all the different shapes of flow straighteners considered whether they were tested in fully developed or uniform flow.

Plotting the mean value of ε between 0 and 4° against the length of the flow straightener, Fig 7 is obtained. The shape of the graph is hardly affected by the sign of the swirl.

Explanation of experimental results in the light of existing theory

None of the present turbine flowmeter theories is sufficient to explain all the results obtained here. The theory by Hochreiter[3] is insensitive to Reynolds number effects as his theory is assumed to hold at 'high' Reynolds number. It will thus always give a horizontal calibration curve.

Lee and Karlby's[1] theory also cannot explain the results because the turned down and full-diameter rotor meters are working at the same Reynolds number. They have roughly the same dimensions and yet their calibration curves (Fig 2) are very different.

In the theory proposed by Rubin *et al.*[4] only the driving torque is considered, although the authors agree that the knowledge of the retarding torque is also essential to understand fully the mechanism of the turbine flowmeter. As their upstream profile is assumed to be uniform this theory is also inadequate.

Jepson's theory[2] was specifically designed to obtain the effect of profile change from a uniform to a fully developed flow. It is not suitable to explain what takes place in meters in general, and the results obtained here in particular, because the predicted calibration curves will always be horizontal lines.

Tan and Hutton[5] tried to explain the rising flowmeter characteristic with decreasing flowrate using aerofoil theory and the effect the leakage flow at the blade tip. In more recent work by Fakouhi, reported by Scott[6], the theory was extended to explain the viscosity effect. Although Tan's theory is quite a comprehensive approach, it failed to take the effect of upstream velocity profile changes into consideration. Salami[7] showed that the flow in the entry portion of a test pipe could be complicated as the boundary layer for a given meter position could be laminar at the lower flowrates and either laminar, transitional or turbulent at the higher flowrates even though the core of the developing flow still remains almost constant. These changes in the boundary layer affect the velocity just upstream of the meter.

Velocity traverse

To ascertain why the existing theories failed to explain the author's measurements, the velocity profile was traversed by a pitot tube, used in conjunction with wall static pressure tappings, at the three flowrates used above for the upstream profile effect. The following points emerged:

Table 1 Flow straightener designs investigated

	Length, mm				
Straightener type	12.7	25.4	38.0	50.8	76.2
Vaned					
4 Vanes	*	*	*	*	*
6 Vanes	*	*		*	
8 Vanes	*	*		*	
Ringed					
4 Rings	*	*		*	

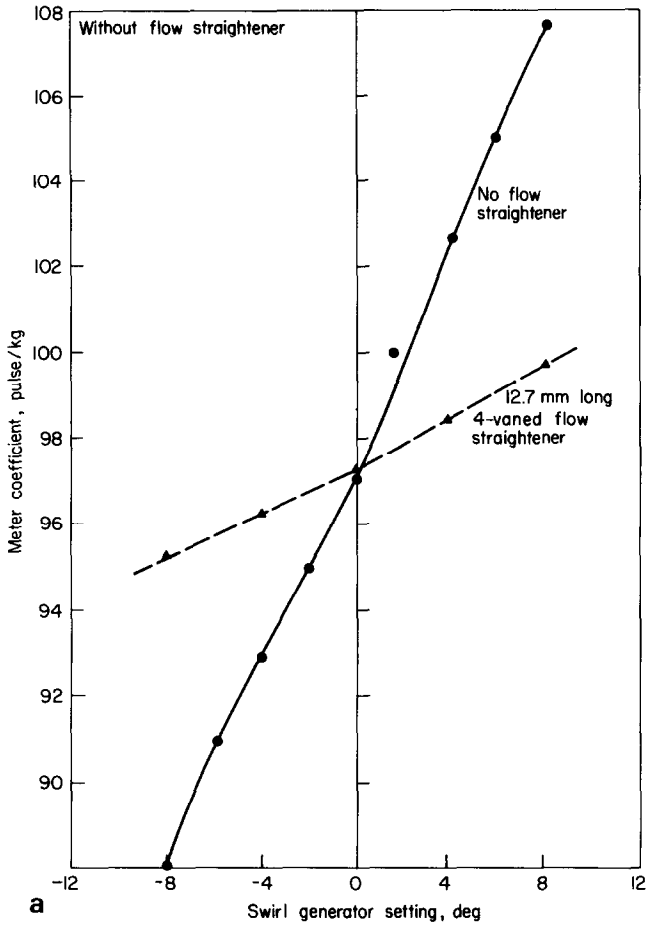

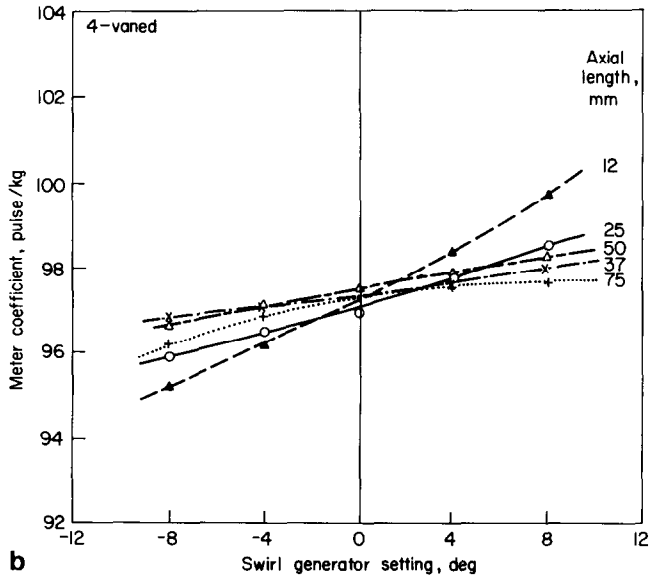

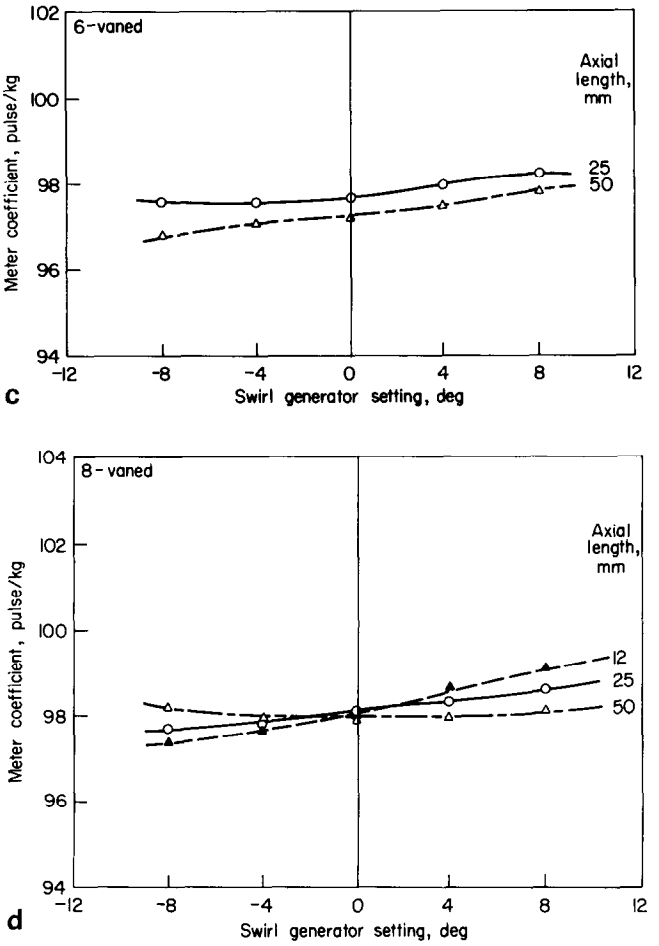

Fig 6 Swirl effect on meter coefficient for various generator settings, with no flow straightener and with various lengths of vaned straighteners

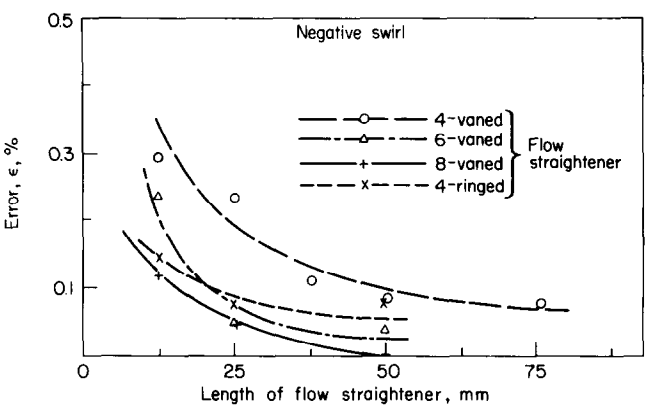

Fig 7 Reduction in the error due to swirl with various flow straighteners for negative swirl upstream

1. It is not possible to obtain completely uniform flow in this rig because there is a thin boundary layer about $0.025d$ thick just after the reducing piece.
2. In fully developed pipe flow the velocity profile becomes peakier as the Reynolds number is decreased; the same trend is also obtained for developing pipe flow. For instance, the uniform potential core velocity at the entry section increased from 1.009 at the highest flowrate to 1.040 at the lowest flow relative to the mean velocity U_0.
3. The law:

$$\bar{U} = \left(\frac{y}{\delta}\right)^{1/n} \tag{1}$$

correlates the data for the traverses very well, especially for the medium and highest flowrates.
4. The experiment confirms what is already evident in Jepson's work[2], that fully developed flow occurs at several pipe diameters after the section where the boundary layer first reaches the pipe centre. At the

latter section the value of n is generally smaller than when the flow is fully developed, thus suggesting a flow re-distribution between the two sections. More details of the results of these traverses are given elsewhere[8].

New theoretical model

Since the experiments described below were all made on the same meter, albeit turned down to give anther tip clearance, a good theoretical model should give quite accurate predictions of the meter coefficient when the appropriate flow conditions, eg swirl distribution, profile distribution, etc, are inserted. A computer model is proposed so that the appropriate flow condition can be inserted without over-simplifying the model. The model recognizes:

(1) That the velocity distribution upstream of the meter is not necessarily uniform. The velocity U_r just ahead of the leading edge of the rotor may not be exactly that obtained from the pitot traverse because it will be affected by the hub of the meter and the blockage and rotation of the rotor.

The meter hub is assumed to increase the velocity in the potential core uniformly without changing the wall boundary layer thickness. Some of the fluid displaced by the hub appears in the boundary layer causing the exponent of the power law near the wall to be slightly increased. Note that when the hub-to-tip ratio is very high, this process makes the exponent near the wall so high that one obtains an almost uniform flow irrespective of the velocity distribution just before the hub. This effect makes the increase in the potential core, or the central position when the boundary layer has reached the hub, slightly smaller than that given by a straightforward increase of the velocities over the section due to the flow displaced by the hub.

Although the hub of the meter is small the rotor will still affect the flow, but by how much is the problem. The area blockage at the rotor hub periphery due to the blade is about 0.2 (area blockage due to the rotor at a given radius r is defined as $Nt/2\pi r$) decreasing to about 0.025 at the blade tip and it is not clear how this type of variation will affect the axial flow distribution. It should be pointed out that the effective blockage of the rotor, which is the flow displaced by the rotor to the total flow, is slightly greater than that given by the area ratio of the rotor to the meter internal area when the developing pipe flow is not uniform. This is because the rotor is situated in the region of highest velocities in the pipe. The difference between the area and the effective blockages rises to about 0.5% on the total flow when the meter is in fully developed pipe flow.

Finally, the rotation of the rotor may cause a centrifugal force to be set up which will tend to re-distribute the axial velocity and consequently there will be no radial equilibrium. It is possible that the redistribution can affect the blockage effect of the rotor. The re-distribution is also likely to be a function of the rotational speed of the rotor and the viscosity of the fluid.

(2) That the flow may not necessarily be swirl-free. However, the swirl distribution must be capable of being described mathematically.

(3) That while the flow is non-uniform it may not be possible to keep the angle of attack, a, small and the angle may even go negative especially in fully developed flow. From the limited data available for flat plates[9,10], it is seen that C_D is sensitive to the angle of incidence. Consequently, the coefficient of drag will most likely change along the blade length. A quadratic has been fitted to the mean of these curves and is:

$$C_D/C_{Do} = 0.045a^2 + 0.104a + 1.0 \tag{2}$$

Also, from the data of Riegels[9] and Betz[10] it is seen that C_{Do} has no recognizable trend with Reynolds numbers, and consequently will be assumed constant for all flowrates.

(4) That there will be a distribution of lift along the blade length which will not necessarily be uniform. The lift distribution will cause trailing vortices to be shed which will then reduce the angle of attack by the induced angle a_i. Broadly speaking this flow process is similar to that in wings with finite span[11] and as such a_i can be assumed to be given by[12]:

$$a_i = \frac{C_L}{F(AR,\tau)}$$

where AR is the aspect ratio and τ the geometry of the blade. Assuming that the angle of attack is small, the effective lift parameter $dC_L/da(=m_e)$ can be shown to be given by:

$$m_e = \frac{m}{1 + \dfrac{1}{F(AR,\tau)}}$$

or simply:

$$m_e = \frac{m}{1 + \dfrac{1}{F}} \tag{3}$$

where m is the two-dimensional lift parameter for a flat plate and is equal to 2π. F will be assumed to remain constant for a given rotor.

(5) That the bearing drag may not be small especially at very low flowrates. A journal-type bearing is assumed because in the miniature ball bearing used in the present meter it is likely that the friction drag of the ball on the cage will far outweigh the contact friction of the balls on the housing. The liquid being metered is assumed to lubricate the bearing. Thus, the bearing torque T_b is proportional to the meter rotational speed ω_R and the fluid viscosity, μ, ie:

$$T_b \propto \omega_R \mu \propto \frac{U_0^2 \rho}{Re}$$

giving:

$$T_b = \frac{k \rho U_0^2 R_0^3}{Re} \tag{4}$$

where k is a constant.

(6) That there may be leakage losses at the blade tip. Leakage here simply means the flow that bypasses the meter rotor through the clearance between the rotor and the housing. There are two sources of leakage flow. First, the direct leakage flow which is the amount of liquid which lies in the clearance space and is determined by the dimension of the clearance and the velocity profile just upstream of it. The second source is the leakage flow caused by the 'retained lift' at the blade tip which induces

flow at right-angles to the blade chord[13] when the clearance is small. The retained lift is assumed to be proportional to the angle of attack at the blade tip, a_t, but diminishes with the clearance width. The leakage flow will depend on the magnitude of the force propelling the fluid through the small clearance and the resistance of the clearance. The force will be assumed to be proportional to the retained lift and the resistance to the viscosity, μ, of the liquid, being metered.

As the direct leakage flow will be taken care of by the limits of integration in the turbine meter formula given below, the leakage flow from now on will refer to the induced leakage flow only and is given by:

$$V_L = f(\mu, C_L) = f(\mu, a_t, U_0^2) \tag{5}$$

If the profile near the blade tip is almost constant with flow for a given liquid then:

$$V_L = \bar{B} U_0^2$$

and therefore, the torque loss T_s due to the liquid bypassing the rotor is: $T_s = B U_0^2$

It is possible that there could be additional losses, for example pick-up torque losses in meters with magnetic pick-up circuits, but these will be assumed to be secondary losses and as such varying with the square of the mean velocity, U_0.

Thus a general turbine flowmeter formula can be derived (Appendix):

$$\int_{\bar{r}_h}^{\bar{r}_t} \left[\left(\frac{m}{1+1/\bar{F}} \right) \left\{ \frac{2\pi R_0 \bar{r}^2 \bar{U}^2}{p} - (W - W_{sr}) \bar{r}^2 \bar{U} \right\} - C_{Dr}(W - W_{sr}) \bar{r}^2 \bar{U} \left(\left\{ 1 + \left(\frac{W - W_{sr}}{\bar{U}^2} \right)^2 \bar{r}^2 \right\} \left\{ 1 + \left(\frac{2\pi R_0}{p} \right)^2 \bar{r}^2 \right\} \right)^{1/2} \right] d\bar{r} - \frac{k}{N\bar{l}Re} - \frac{B}{N\bar{l}} = 0 \tag{7}$$

where B is a constant for all the secondary losses but is largely due to the leakage loss. It can be seen that the shape of the calibration curve will not be affected if B is assumed constant and thus could be ignored.

Computational method

In the computation the bearing loss is assumed to be small except for flowrates below quarter of the maximum flowrate used. The secondary losses are ignored for the reason stated above. Finally, the flow is assumed to be swirl free, hence $W_{sr} = 0$.

Given the boundary layer thickness δ, and the corresponding value of n for a given test section and test condition, the non-dimensional velocity distribution across the section is immediately obtained from Eq (1) and:

$$\frac{U_0}{U_c} = \left(1 - \frac{\delta}{R_0} \right)^2 + 2 \left[\frac{n}{n+1} \frac{\delta}{R_0} - \frac{n}{2n+1} \left(\frac{\delta}{R_0} \right)^2 \right] \tag{8}$$

obtained by integrating Eq (1) over the pipe section; U_c is the potential core velocity. The distribution is equivalent to the one obtained by pitot traverse. The distribution is then corrected for the hub effect, as explained above, by reducing the area blockage effect of the hub $(A/(A - A_h))$ on the potential core velocity by 0.003. The constant 0.003 is obtained by noting that only the turned down rotor in the almost uniform flow will be sensitive to this modification because its rotor lies wholly in the potential core. Without this modification there is a discrepancy for the maximum flow of about 0.3% in the theoretical predictions obtained for this rotor between the uniform and the fully developed flow which did not exist in the experimental result of Fig 2. The constant eliminates this discrepancy but does not affect the predictions for the full-diameter rotor meter. The constant will diminish with hub ratio ψ and will approach zero as the hub size becomes so large that the boundary layer thickness almost vanishes.

Next, the blockage effect of the rotor is taken into consideration to give the actual velocities to be used in the integrands of Eq (7). The most satisfactory explanation of this blockage effect is that the rotor changes the velocity at a point just upstream by an amount equal to its peripheral blockage at that point. However, because of its rotation this blockage is reduced by a function of the speed, B_g. Thus:

$$U_r = \frac{U_r}{1 - \left(\frac{Nt}{2\pi r} \right) B_g} \tag{9}$$

where $Nt/2\pi r$ is the peripheral blockage of the rotor.

The value of B_g is inferred thus: when the calibration curves for both meters were predicted using U_r^* or even $U_r^*/(1 - (Nt/2\pi r))$ for the fully developed flow there was a slight rise in the turned-down rotor and a slight drop in the full diameter rotor meters relative to the corresponding experimental calibration curves as the flow decreased. These discrepancies were almost eliminated by using $B_g = 0.7 - 0.5\ (\omega_R/\omega_{R^*})$ (Fig 2). Similar discrepancies which existed in the almost uniform flow were even more drastically reduced by this empirical assumption.

Finally, the non-dimensional meter coefficient, W, is computed. A value of W of about unity is arbitrarily chosen and the angle of attack is obtained from knowledge of the blade pitch. The coefficient of drag is evaluated from Eq (2) and the integrand in Eq (7) obtained by using Simpson's rule and about 1000 blade elements. If the integrand is not zero the value of W is either increased or decreased until this condition is fulfilled and the value of W then gives the meter coefficient. Provided $F > 0.5$ the value of W is not considerably affected by F.

Results from the theoretical model

Fig 8 has been obtained for the upstream velocity profile effect using only the expression for the driving torque, ie the integrand in Eq (7) with $C_{Dr} = 0$ and the results of the pitot tube traverse unmodified either by the meter hub or the rotor blockage effects. The similarity between this figure and the experimental results in Fig 3 is quite obvious. This shows the importance of the upstream velocity profile on the meter coefficient, one of the main points of this paper.

The theoretical figures above have the same basic fault, ie that when the boundary layer is thin the results for both meters have to be decreased considerably for the smallest flowrate and by a little for the medium and highest flowrates. This strongly suggests modification of the pitot tube traverse result both by the hub and the meter rotor.

The theoretical predictions derived using the modifications suggested above are shown in Fig 9. The small

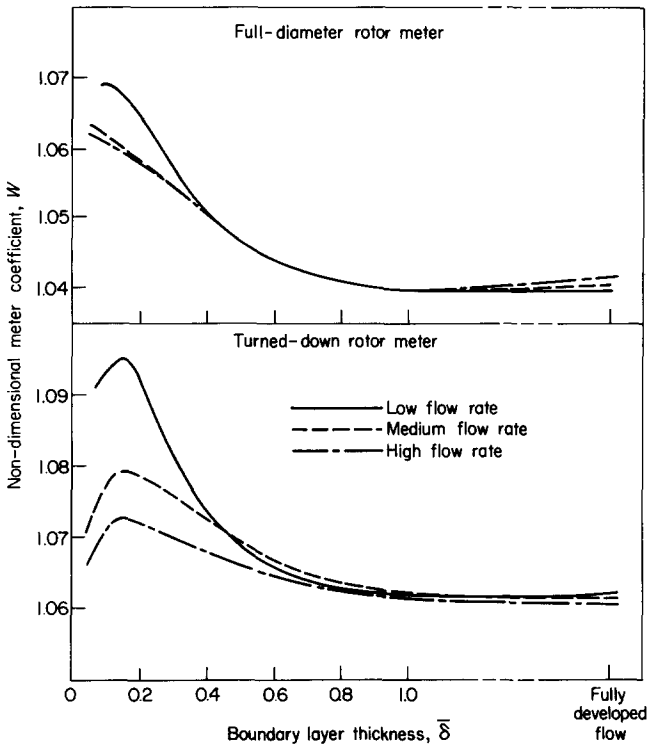

Fig 8 Theoretical prediction of turbine meter upstream profile effect. The result of the pitot traverse has been used unmodified and the first two integrands in Eq (7) and other terms have been ignored. Note the similarity between the above curves and Fig 3

discrepancies which exist in this Figure and in Fig 2 can be explained by the induced leakage effect as follows.

From Eq (7) it is seen that if leakage flow was not ignored, the meter coefficient would be lower than the theoretical values plotted in Fig 9. Where the angle of attack at the blade tip is high the leakage flow will also be expected to be high and the drop in the meter characteristic consequently greater. Fig 10 shows the angle of attack along the blade length for the turned down and full-diameter meters calibrated in almost uniform and in fully developed flows for the low and high flowrates. The slight discrepancy between the experimental result and theoretical prediction at the maximum flowrate is due to the increased angle of attack.

Calibration curves

The calibration curves (Fig 2) are special cases of the upstream profile effect discussed above and their shapes are mainly due to the change in the velocity profile with flowrate. The discrepancy between the experimental and theoretical predictions is also due to the leakage flow. The sudden decrease in the curve for the full-diameter rotor meter and the sharp rise in the curve for the turned-down rotor meter at the smallest flow in the fully developed regime is attributed to the fact that the pipe-flow may be approaching transition to laminar flow.

Results for the commercial meter

The commercial meter showed very little upstream profile effect at a given flowrate as it was moved from the uniform profile to the fully developed flow in the 38 mm diameter test line (Fig 4). As the meter has a high hub-to-tip ratio, $\psi = 0.55$, and the rotor is mounted inside a venturi with 25.4 mm diameter throat, the profile presented to the rotor at a given flowrate will most probably be the same irrespective of the velocity profile in the test length just upstream of the meter and will be almost uniform. Thus, the flow condition and the fact that the meter has a large-tip clearance makes it similar to the turned down rotor meter in the almost uniform flow already studied above. The calibration curve will consequently be expected to rise with flow decrement except at very low flowrates when the bearing effect will make the curve decrease with flowrate. This latter region has not been reached in the curves shown here.

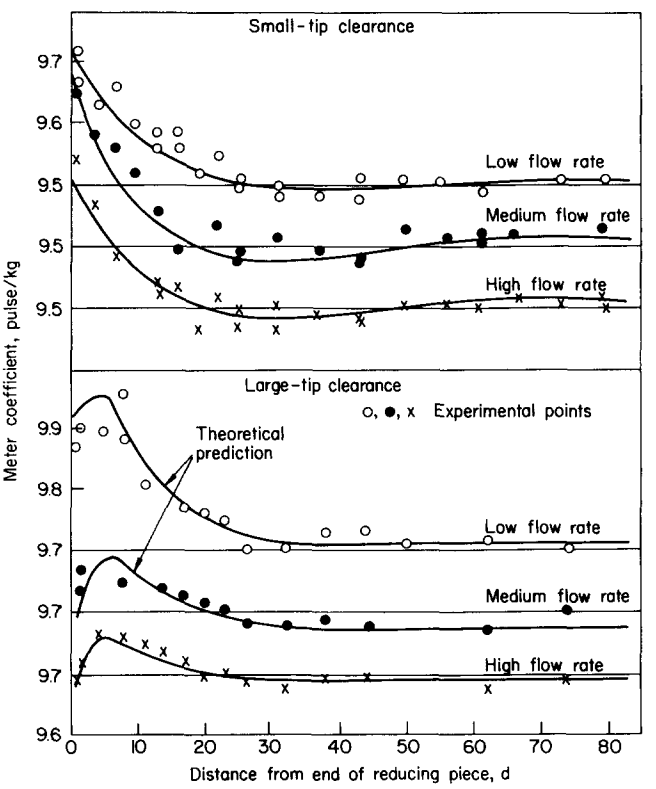

Fig 9 Theoretical prediction of turbine meter upstream profile effect. The X-axis has been shifted for clarity

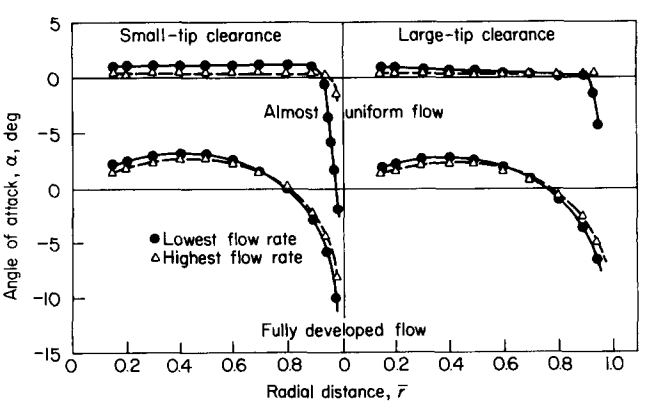

Fig 10 Radial distribution of the angle of attack in almost uniform and fully developed flows

Effect of flow straighteners

From Fig 6, it will be observed that at zero swirl the meter gives different readings with various flow straighteners. This confirms that the presence of the flow straightener affects the meter calibration. The effect of flow straighteners in a swirl free flow will depend on the alignment of the straightener with respect to the pipe axis and the type of velocity distribution after the flow straightener.

The alignment of the flow straightener can affect the meter reading because, although it may remove the swirl in the fluid flowing through it, if it is not properly aligned it may generate some swirl at its downstream end. However, this will not be serious provided the swirl generated due to misalignment is small and does not vary with flowrate. This is so because there is generally a linear region around zero swirl and the effect of small constant swirl in the flow would be merely to raise or lower the calibration curve parallel to itself. It is, therefore, important that the meters be calibrated individually as the alignment of the flow straighteners may vary slightly from one meter to the other.

For the meters tested here the error, ε, was 1.25% per degree of swirl in a uniform flow and 1.35% in the fully developed flow. Thus the axial velocity distribution will cause a discrepancy of 0.10% per degree in the meter reading if the meter is calibrated in a fully developed flow and is used where the flow is fairly uniform.

The velocity distribution reaching the rotor will depend on the width of the wake behind the flow straighteners. It will, therefore, be dependent on the length and thickness of the flow straightener as well as its distance from the rotor. The number of blades in the flow straightener is also important. In the case of flow straighteners with equally spaced radial vanes the velocity distribution will vary along different radii. Thus along the radius of the pipe just downstream of the vane the velocity will be small, while for radii in between vanes the velocity will be relatively larger. This type of velocity distribution will cause a pulsation in the meter, the frequency of which will vary directly with the product of the speed of the rotor and the lowest common multiple of the number of vanes on the flow straightener and rotor. It is not clear how this velocity distribution will affect the meter calibration or whether it is the frequency of the pulsation or the range of the velocity reaching the rotor that is more important in determining this effect.

Effectiveness of flow straighteners

From Fig 7, the following trend is generally consistent especially near the swirl generator zero setting:

1. For any set of flow straighteners, the effect of swirl on the meter diminishes with increase in the length of the straightener.
2. For the various sets of flow straighteners tested with equally spaced radial vanes, the effect of swirl diminishes with the increase in the number of vanes in the straightener when the length is the same.

Other noteworthy points are that all the graphs generally show a rapid decrease around straightener lengths of 12.5 and 25 mm but decrease more gradually thereafter. It also appears that the flow straightener with four tubes is just as effective in removing swirl as the six radial-vane type.

Mathematically, the error, ε, of the meter from the above can be expressed as:

$$\varepsilon = F_1(N_s) \times F_2(L_s) \tag{10}$$

where $F_1(N_s)$ is a function of the number of vanes in the flow straighteners and $F_2(L_s)$ a function of the length. By trial and error it is found that:

$$\varepsilon = F_s(N_s^{3/2} L_s/d) \tag{11}$$

where F is dependent on the swirl distribution, the upstream velocity profile, the vane thickness, the type of flow straightener and the meter design. L_s/d is the non-dimensional flow straightener length.

Using the average error ε, Fig 11 has been drawn for the upstream and downstream positions. The correlation is fair.

From Eq (11) it can be seen that the number of blades has more impact on the effectiveness of flow straighteners, as far as a turbine flowmeter is concerned, than the length. Thus, for a given ineffective flow straightener, doubling the number of vanes is much better than doubling the length.

Flow straighteners generally remove swirl by dividing the incoming swirl into smaller swirls that then go into the channels of the straighteners. During their passage through the channel the circular motion is reduced or destroyed completely by friction. After leaving the flow straightener the residual swirls, if any, combine and then affect the meter reading. If the channels of the flow straighteners are too large, then it requires a much longer length to destroy the swirl completely. From the correlation presented here, the lengths of 4- and 3-vaned straighteners to remove swirl will be about 150 and 250 mm respectively. If on the other hand the flow passages are too small, excessive flow losses may result.

Small swirls of up to 4° have been used for the correlation because at higher swirl the axial velocity profile is disturbed due to the type of swirl generator used.

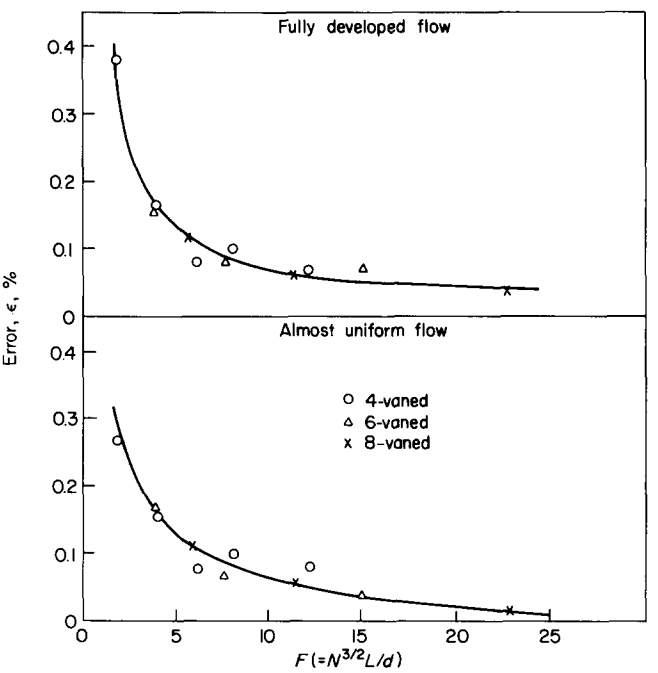

Fig 11 Correlation of flowmeter effectiveness in terms of F *for uniform and fully developed flows*

If the axial velocity of flow before the swirl generators is uniform it leaves the generator with the velocity near the centre smaller and that near the wall higher than the mean velocity. This distribution of velocity normally results in an increased meter coefficient. Consequently, the change in meter characteristics in the region $+4°$ to $+8°$ is usually greater than for the $0°$ and $+4°$ setting. On the other hand, the change in the meter characteristics between $-4°$ and $-8°$ is lesss than that between 0 and $-4°$. The reason for this is that between $4°$ and $8°$ the change in meter characteristics caused by velocity change and swirl assist one another while between $-4°$ and $-8°$ they oppose each other.

The above is well illustrated by the result for the 8-vaned flow straightener (Fig 6). It is the only flow straightener that completely removed the swirl between the $-4°$ and $+4°$ swirl setting. However, the axial velocity has been disturbed in an identical manner in the region $-4°$ to $-8°$ and $+4°$ to $+8°$, and consequently the meter characteristics rise by almost the same amount in these regions.

Most of the above conclusions and correlations were also obtained with the experiment carried out in the fully developed flow towards the end of the test line. However, for high values of F the errors are slightly larger than these for the upstream position thus indicating that the flow straightener is slightly less effective in fully developed flow.

Conclusion

The turbine flow meter model proposed can be summarised as follows:

The velocity profile in the pipe becomes peakier, ie the percentage of the flow passing through the central pipe region becomes greater as the flow is decreased. The meter responds to this change in upstream profile and consequently a meter with large-tip clearance generally has a meter coefficient which rises as the flowrate decreases because the blade profile loss does not play a major role except in highly viscous liquids.

For meters with small-tip clearance, eg the full-diameter rotor meter, this profile change does not have much effect because whatever increase there is in the percentage of the flow going through the pipe centre is almost completely nullified by the decrease in flowrate near the blade tip. Moreover, the angle of attack at the blade tip is quite high and becomes progressively higher with decreasing flowrate. The consequent increase in drag over the complete blade length and the increase in the leakage flow accounts for the decrease in meter coefficient with decrease in flowrate for this type of meter.

The velocity profile actually reaching the rotor is modified by both the blockage effect of the hub and the rotor blades, as well as the rotation of the latter.

At very low flowrates the bearing torque will be large compared with the driving torque and eventually the meter coefficient will decrease with decreasing flowrate irrespective of the rotor geometry. The experiments here have been carried out in water but when a very viscous liquid is used the rotor loss may overshadow the upstream profile effect because it is so large. Rotor loss may thus be the most important factor in determining the shape of the calibration curve for high viscosity fluids.

The investigation also shows that the presence of the flow straightener affects the meter characteristics whether there is swirl or not. As this effect depends on uncertainties such as its alignment with respect to the pipe axis, it may be difficult to take this into account in theoretical models.

As we have seen, the effectiveness of the flow straighteners in removing swirl depends on the type of flowmeter as well as its length. A correlation has been proposed here for the radial-vaned flow straighteners used but the correlation will generally depend on factors such as the type of flow straightener and the meter design. However, the author believes that such a correlation can always be found for any turbine flowmeter and can be useful in the design of a meter. The effectiveness of a flow straightener made out of four equal rings in removing swirl is almost the same as that for a 6-radial vaned straightener.

Acknowledgement

The author is grateful to Professor S. P. Hutton, who supervised the project, for his encouragement and to the entire workshop staff of the Mechanical Engineering Department at the University College, Cardiff, where the project was undertaken.

References

1. **Lee W. F. Z. and Karlby H.** A study of viscosity effects and its compensation on turbine-type flowmeter. *Trans. ASME J. Basic Engng. 1960*, **82**, *71?–727*
2. **Jepson P. and Bean P. G.** Effect of upstream velocity profiles on turbine flowmeter registration. *J. Mech. Engng. Sci. 1969*, **11**, *503–510*
3. **Hochreiter H. M.** Dimensionless correlation of coefficients of turbine-type flowmeters. *Trans. ASME 1958*, **80**, *1363–1368*
4. **Rubin M., Miller R. W. and Fox W. G.** Driving torque in a theoretical model of a turbine meter. *Trans. ASME J. Basic Engng. 1965*, **87**, *314–320*
5. **Tan P. A. K. and Hutton S. P.** Experimental analytical and tip clearance loss studies in turbine-type flowmeter. *Proceedings of International Conference on Modern Developments in Flow Measurement, Harwell 21–23 September 1971 (Ed. C. G. Clayton) Peter Peregrinus Ltd, London, 1972, pp. 321–346*
6. **Scott R. W. W.** Development in flow measurement I, *Applied Science Publishers, 1982, pp. 186–192*
7. **Salami L. A.** Towards standardization of turbine-type flowmeters, *Proceedings of International Conference on Advances in Flow Measurement Techniques, University of Warwick, England, 9–11 September 1981, BHRA Fluid Engineering, 1981, pp. 279–282*
8. **Salami L. A.** Effect of velocity profile just upstream of a turbine flowmeter on its characteristics, *Southampton University Rep. ME/72/2*
9. **Riegels F. W.** Aerofoil Sections, *1961, Butterworth, London*
10. **Betz Z.** *Introduction to the Theory of flow machines, 1st edition (Pergamon Press, Oxford), 1966*
11. **Lakshminarayana B. and Horlock J. H.** Secondary flows and losses in cascades and axial flow turbomachines, *Int. J. Mech. Sci. 1963*, **5**, *287–307*
12. **Dommarsch D. O., Sherby S. S. and Connoly T. F.** *Airplane Aerodynamics, 4th edition (Pitman Publishing Corporation, New York), 1967*
13. **Lakshminarayana B. and Horlock J. H.** Tip clearance flow and losses for an isolated compressor blade, *A.R.C. Rep. and Memorandum, 1962, 3316*

Appendix. Theoretical method

When the meter is rotating steadily the driving torque, T_d, just balances the retarding torque made up of the bearing torque, T_b, and the torque due to secondary loss T_s. Thus:

$$T_d = T_b + T_s \tag{12}$$

It is the retarding torques on the right-hand side of Eq (12) which actually determine the exact speed of rotation of the meter.

Now, with the nomenclature in Fig 12 the net driving torque is the sum of the resolved components of the lift and drag forces in the tangential direction. Thus, considering a blade element at a radial distance r, the driving torque dT_d is given by:

$$dT_d = Nr(L_r \cos\beta - D_r \sin\beta)$$

where N is the number of blades on the rotor and subscript r refers to the radial position of the element being considered.

$$L_r = \tfrac{1}{2}\rho \bar{V}_r^2 C_{Lr} c\,dr$$
$$D_r = \tfrac{1}{2}\rho \bar{V}_r^2 C_{Dr} c\,dr$$
$$dT_d = \tfrac{1}{2}N\rho \bar{V}_r^2 c(C_{Lr}\cos\beta - C_{Dr}\sin\beta)r\,dr$$

Now:

$$C_L = m\sin(a - a_1) = m\sin a$$

Therefore, from Eq (3), which takes the effect of the induced angle into account:

$$C_L = m\sin(\phi - \beta)/\left(1 + \frac{1}{F}\right)$$

Therefore:

$$\bar{V}_r = U_r/\cos\beta$$
$$c = 1/\cos\phi$$
$$\tan\phi = 2\pi r/p$$

Thus:

$$dT_d = \frac{N\rho U_r^2 l}{2\cos^2\beta\cos\phi}\left(\frac{m\sin a\cos\beta}{1+\frac{1}{F}} - C_{Dr}\sin\beta\right)r\,dr$$

$$= \frac{N\rho U_r^2 l}{2}\left(\frac{m\sin a}{\cos\beta\cos\phi}\frac{1}{(1+1/F)} - C_{Dr}\frac{\tan\beta}{\cos\beta\cos\phi}\right)r\,dr \tag{13}$$

Now:

$$\frac{\sin a}{\cos\beta\cos\phi} = \frac{\sin(\phi-\beta)}{\cos\beta\cos\phi}$$
$$= \tan\phi - \tan\beta$$
$$= \frac{2\pi r}{p} - \frac{\omega_r . r}{U_r}$$

where p is the pitch of the blade helicoid, the same for all points, and ω_r the tangential angular velocity of the blade element minus the swirl velocity. From Fig 12 it is also clear that:

$$\frac{\tan\beta}{\cos\beta\cos\phi} = \frac{\omega_r . r}{U_r}\sqrt{\left\{1+\frac{(\omega_r . r)^2}{(U_r)}\right\}\left\{1+\frac{(2\pi r)^2}{(p)}\right\}} \tag{14}$$

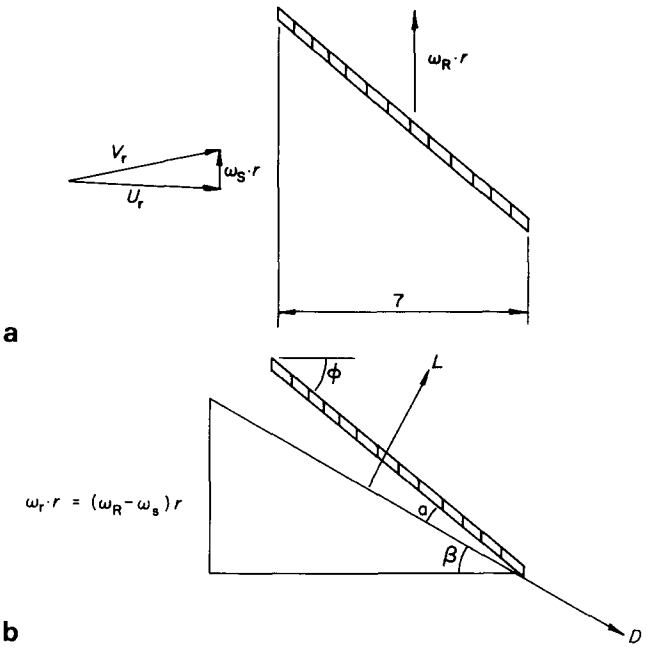

Fig 12 Development of the velocity triangle for a turbine-type flowmeter with swirl in the flow at entry (b) and from absolute velocities (a)

Thus:
$$T_d = \int_{r_h}^{r_t} \frac{N\rho U_r^2 l r}{2}\left[\frac{m}{\left(1+\frac{1}{F}\right)}\left(\frac{2\pi r}{p} - \frac{\omega_r . r}{U_r}\right) C_{Dr}\frac{\omega_r . r}{U_r}\sqrt{\left\{1+\frac{(\omega_r r)^2}{(U_r)}\right\}\left\{1+\frac{(2\pi r)^2}{(p)}\right\}}\right]dr \tag{15}$$

From Eqs (4) and (6):

$$T_d = T_b + T_s = \frac{\bar{\bar{K}}\rho U_0^2 R_0^3}{R_e} + \bar{\bar{B}}U_0^2 \tag{16}$$

Therefore, non-dimensionalising the velocity and the lengths by U_0 and R_0 respectively:

$$\bar{r} = \frac{r}{R_0}, \quad \bar{l} = \frac{1}{R_0}, \quad \bar{U}_r = \frac{U_r}{U_0}$$
$$W = \frac{\omega_R R_0}{U_0}, \quad W_{sr} = \frac{\omega_s R_0}{U_0} \tag{17}$$

Substituting Eqs (16) and (17) into Eq (15) gives the general turbine flowmeter formula:

$$\int_{\bar{r}_h}^{\bar{r}_t}\left[\frac{m}{\left(1+\frac{1}{F}\right)}\left\{\frac{2\pi R_0}{p}\bar{r}^2\bar{U}_r^2 - (W - W_{sr})\bar{r}^2\bar{U}\right\} - C_{Dr}(W - W_{sr})\bar{r}^2\bar{U}\left(\left\{1+\frac{(W-W_{sr})^2}{\bar{U}^2}\bar{r}^2\right\}\left\{1+\left(\frac{2\pi R_0}{p}\right)^2\bar{r}^2\right\}\right)^{1/2}\right]d\bar{r} - \frac{K}{N\bar{l}R_e} - \frac{B}{N\bar{l}R_0^3} = 0$$

W in the above equation is the non-dimensional form of the meter coefficient as the numerator $\omega_R . R_0$ (see appropriate expression in Eq (17)) can be converted to pulse/s and U_0 to kg/s.

The solution of Eq (18) for W gives the meter coefficient and can be used to obtain the effects of the axial velocity profile, the swirl and possibly the viscosity on the meter coefficient.